

HIGH-RESOLUTION 4.7 MICRON KECK/NIRSPEC SPECTROSCOPY OF THE CO EMISSION FROM THE DISKS SURROUNDING HERBIG Ae STARS

GEOFFREY A. BLAKE¹ AND A. C. A. BOOGERT²

Received 2003 December 3; accepted 2004 March 18; published 2004 April 8

ABSTRACT

We explore the high-resolution ($\lambda/\Delta\lambda = 25,000$; $\Delta v = 12 \text{ km s}^{-1}$) M -band ($4.7\text{--}5.1 \mu\text{m}$) spectra of several disk-dominated Herbig Ae (HAe) systems: AB Aur, MWC 758, MWC 480, HD 163296, and VV Ser. All five objects show $^{12}\text{CO } v = 1\text{--}0$ emission lines up to $J = 42$, but there is little or no evidence of moderate- J , $v = 2\text{--}1$ transitions despite their similar excitation energies. AB Aur shows ^{13}CO emission as well. The line/continuum ratios and intensity profiles are well correlated with inclination, and they trace collisionally driven emission from the inner disk ($R_{\text{th}} \lesssim 0.5\text{--}1 \text{ AU}$) as well as resonance fluorescence to much larger radii ($R_{\text{fr}} \lesssim 50\text{--}100 \text{ AU}$ for $J \lesssim 10$). The temperature, density, and radiation field profiles required to fit the CO emission are in good agreement with models of HAe disks derived from their spectral energy distributions. High-resolution and high dynamic range infrared spectroscopy of CO, and future observations of less abundant species, thus provide direct access to the physicochemical properties and surface structure of disks in regions where planet formation likely occurs.

Subject headings: infrared: ISM — ISM: molecules — planetary systems: protoplanetary disks — stars: formation

On-line material: color figure, machine-readable table

1. INTRODUCTION

As the means by which angular momentum and matter are exchanged between molecular clouds and young stars and as the birth sites of planets, circumstellar disks provide the pivotal link between star formation and (exo)planetary science. The spatiotemporal properties of disks, as gleaned from their spectral energy distributions (SEDs), are similar to those of the solar nebula (Beckwith et al. 1990; Skrutskie et al. 1990) but have been verified for only a *handful* of objects. With optical/infrared (IR) imaging (Krist et al. 2000) and, especially, interferometry (Monnier & Millan-Gabet 2002) we have begun to probe closer to the central stars but cannot examine critical disk properties such as the surface density or velocity fields, while with current millimeter arrays we can only probe gas beyond 50–100 AU (Dartois, Dutrey, & Guilloteau 2003).

The discovery of extrasolar “hot Jupiters” some 0.05 AU from their parent stars (Marcy, Cochran, & Mayor 2000) has highlighted the central role of star-disk-protoplanet interactions and demands tools that can investigate the critical planet-forming zone of disks. Only high-resolution rovibrational spectroscopy with large format echelle spectrographs permits us to access the inner disk physical conditions and velocity fields at present (Carr, Mathieu, & Najita 2001; Brittain & Rettig 2002). Indeed, the potential kinematic signatures should be readily detectable: Jupiter induces a stellar wobble of only $v_{\text{Dop}} \sim 13 \text{ m s}^{-1}$ for G stars, while $v_{\text{Keplerian}} \sim 13 \text{ km s}^{-1}$ at 5 AU.

CO is widespread throughout the disk (and any surrounding envelope) thanks to its stability, and as the most abundant molecule after H_2 , it forms the natural first step in the high-resolution IR spectroscopy of young stars. Spectra of the CO vibrational fundamental near $4.67 \mu\text{m}$ are especially complementary to pure rotational studies because both gaseous and solid-state CO can be detected in absorption for embedded or

edge-on systems (Boogert, Hogerheijde, & Blake 2002b; Pontoppidan et al. 2003).

Models of inclined, isolated Herbig Ae (HAe) and T Tauri star (TTs) disks (Chiang et al. 2001; Dullemond 2002) predict conditions under which CO emission should occur, as has recently been observed (Brittain et al. 2003; Najita, Carr, & Mathieu 2003). We have therefore undertaken an extensive M -band survey of protostars that examines all phases of the star formation process (A. C. A. Boogert & G. A. Blake 2004, in preparation), and we report here on a systematic study of HAe stars of similar spectral type and known inclinations that provides stringent constraints on the physical properties and velocity fields of disks over radii of 0.5–50 AU. In § 2 we summarize the observations, and the results are presented in § 3. A comparison of the $R = 25,000$ spectra with those predicted by models based on the observed SEDs may be found in § 4.

2. OBSERVATIONS

The Herbig Ae stars AB Aur (spectral type A0), MWC 480 (A5) and 758 (A8), HD 163296 (A1), and VV Ser (A0) were observed with NIRSPEC (McLean et al. 1998) at the Keck II telescope on several observing runs between 2001 January and 2003 July. NIRSPEC was used in the echelle mode with the $0'.43 \times 24''$ slit, providing a resolving power of $R = \lambda/\Delta\lambda = 25,000$ ($\sim 12 \text{ km s}^{-1}$) in two M -band orders separated by $\sim 0.31 \mu\text{m}$. The K -band seeing was typically $\sim 0''.5\text{--}0''.7$.

The data acquisition and reduction procedures are outlined in Boogert, Blake, & Tielens (2002a). Briefly, two nod positions separated by $12''$ were differenced to remove the thermal background, and one-dimensional spectra extracted and wavelength-calibrated via sky emission lines. Corrections for the atmosphere and instrument used nearby standard stars (HR 1620 [A7 V] and HR 6175 [O9 V]) whose H I lines were fitted with Kurucz model atmospheres.

Except for CO transitions with $J > 25$ that are not excited in the Earth’s atmosphere, it is the small imperfections in the cancellation of the many telluric lines that limits the achievable dynamic range for these bright objects. Typical values are

¹ California Institute of Technology, Division of Geological and Planetary Sciences, Mail Stop 150-21, Pasadena, CA 91125; gab@gps.caltech.edu.

² California Institute of Technology, Division of Physics, Mathematics, and Astronomy, Mail Stop 105-24, Pasadena, CA 91125; acab@astro.caltech.edu.

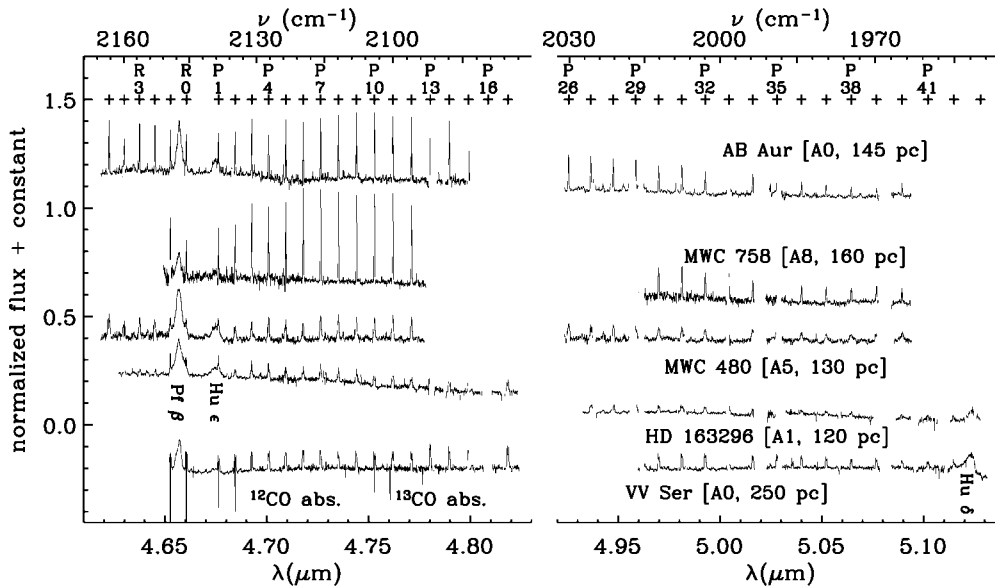


FIG. 1.—Observed, unsmoothed, $R = 25,000$ M -band spectra of Herbig Ae stars, with the gas-phase line frequencies of ^{12}CO indicated by crosses and the H I Pf β , H II ϵ , and H II δ recombination lines labeled. The *Hipparcos*-based distances have uncertainties of ± 20 pc for AB Aur, MWC 480, and HD 163296 and ± 50 pc for MWC 758 and VV Ser (van den Ancker, de Winter, & Tjin A Djie 1998; VV Ser from Chavarría et al. 1988).

greater than 50 but regularly well over 100 for integration times of ~ 4 minutes/echelle setting. Runs throughout the year provided varying Doppler shifts and an effective transmission of $\geq 50\%$ at all velocities of interest (typically, $-30 \text{ km s}^{-1} < v_{\text{Dop}} < 40 \text{ km s}^{-1}$), although some small gaps remain in the spectra, particularly in the R -branch.

The individual echelle orders were combined by applying relative multiplication factors, with the highest orders ($\lambda > 4.90 \mu\text{m}$) aligned by extrapolating a linear fit to the lowest orders. Finally, the spectra have been flux-calibrated using the M -band source brightness reported in the literature: $M = 2.90/4.40$ for AB Aur/VV Ser (Hillenbrand et al. 1992), 4.07 for MWC 480 (Chiang et al. 2001), and 4.47/3.14 for MWC 758/HD 163296 (Malfait, Bogaert, & Waelkens 1998).

3. RESULTS

The most obvious characteristic of the HAe M -band spectra is the presence of many emission lines (Fig. 1) identified with the recombination lines of H I (Pf β , H II ϵ , H II δ) and the $v = 1-0$ rovibrational transitions of ^{12}CO . The overall continuum descends with wavelength for all sources over the wavelength range studied (with slopes of $\sim 3\% - 23\%$), in agreement with *Infrared Space Observatory* $R \sim 2400$ spectroscopy (van den Ancker et al. 2000; Chiang et al. 2001). There is no evidence of the solid CO absorption band at $4.67 \mu\text{m}$, indicating the absence of large columns of cold dust along these lines of sight ($A_V \leq 10$; Shuping et al. 2000). Finally, the spatial extent of the continuum and line emission is comparable to a point

source, i.e., to the seeing of $0''.5 - 0''.7$ ($70 - 140$ AU at the distances of these objects).

Gaussian fits to the H I Pf β , and H II ϵ lines at 4.653778 and $4.6725087 \mu\text{m}$ yield characteristic velocity widths of $\sim 200 - 300 \text{ km s}^{-1}$ FWHMs, values much larger than but well correlated with those of CO (see Table 1). The Pf β lines tend to have more emission to the blue of the systemic velocity. This is most clearly seen in HD 163296, which also has high-velocity wings. The red/blue asymmetry has been attributed to infalling gas, although the origin of the wings is less well established (Najita, Carr, & Tokunaga 1996).

Emission lines of ^{12}CO are identified using the HITRAN database (Fig. 1; Rothman et al. 1992); $v = 1-0$ transitions are detected up to $J = 42$, although some are severely affected by poor atmospheric transmission while others are blended with H I (see Table 1 for the CO FWHMs and line fluxes). The CO lines are kinematically resolved and strongly centrally peaked, except for the high ($J > 9$) transitions in HD 163296 and the lines in VV Ser, which are either flat-topped or clearly show double-peaked profiles. For each HAe star, the emission is centered at the v_{LSR} derived from the pure rotational lines of CO (Mannings & Sargent 2000; Thi et al. 2001).

As Figure 2 shows, the CO line/continuum ratios and the emission profiles are clearly correlated with the system inclination, as gleaned from millimeter interferometry (AB Aur/MWC 758 [for which $\Delta v_{\text{FWHM}} \sim 17 \text{ km s}^{-1}$] and HD 163296 [$\Delta v \sim 73 \text{ km s}^{-1}$]; reanalysis of data in Mannings & Sargent 2000 and Thi et al. 2001, MWC 480 [$\Delta v \sim 62 \text{ km s}^{-1}$]; Simon, Dutrey, & Guilloteau 2000), K -band interferometry (AB Aur, VV Ser [$\Delta v \sim 60 \text{ km s}^{-1}$]; Eisner et al. 2003), and direct imaging (HD 163296; Grady et al. 2000). Interestingly, the high- J lines are always broader than those at low J (Fig. 2). There are also hints that a very narrow, unresolved component is present in only the lowest ($J < 3$) levels, especially in HD 163296, although this needs further confirmation.

Close inspection of the AB Aur spectrum shows that several ^{13}CO lines are present as well (Table 1; Fig. 2). The most convincing detections, at $\sim 2.5\%$ of the continuum, are from the $v = 1-0$, $R(3) - R(10)$ transitions, for which the $^{12}\text{CO}/^{13}\text{CO}$ line

TABLE 1
OBSERVED CO LINE PARAMETERS FOR HERBIG AE STARS

Line	Object	Transition ($v = 1-0$)	FWHM (km s^{-1})	Line Flux ^a ($10^{-17} \text{ W m}^{-2}$)	Notes ^b
^{12}CO	AB Aur	$P(2)$	21.0	10.4	2
^{13}CO	AB Aur	$R(13)$	19.8	1.4 (0.2)	

^a 1σ errors for ^{13}CO in parentheses. Upper limits are 3σ .

^b NOTES.—(2) Some telluric residuals. [Table 1 is published in its entirety in the electronic edition of the *Astrophysical Journal*. A portion is shown here for guidance regarding its form and content.]

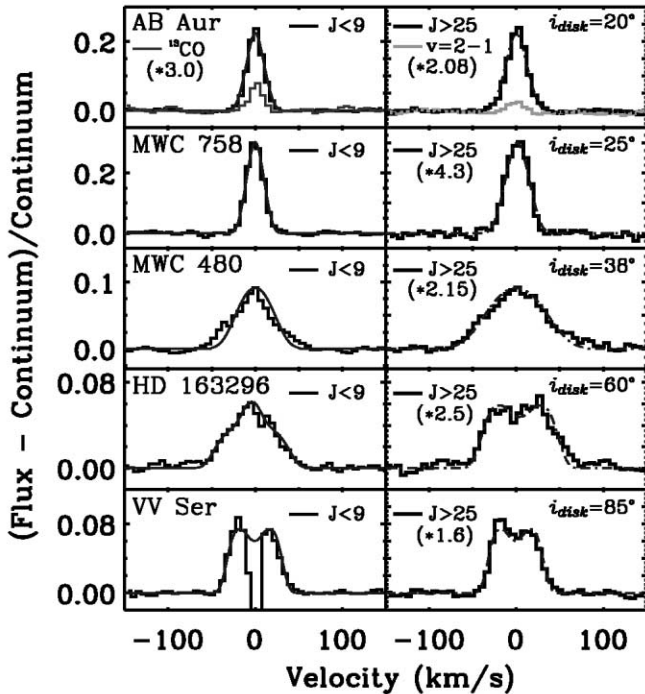


FIG. 2.—CO line profiles, produced by averaging over all low- J levels (left panels) and high- J lines (right panels). The spectra have been normalized to the continuum and shifted to zero flux, and the high- J average was normalized to that at low J by the factor indicated in parentheses. The solid lines depict disk fits to the low- J data, the dash-dotted curves present fits to the high- J transitions. Emission lines from ^{13}CO and ^{12}CO $v = 2-1$ are included for AB Aur. The inclination angles used in the fits are listed in the upper right-hand corner (uncertainties $\pm 5^\circ$ – 10°). [See the electronic edition of the *Journal* for a color version of this figure.]

flux ratio is ~ 8 . Vibrationally excited $v = 2-1$ ^{12}CO emission is tentatively detected in AB Aur at $\sim 1.3\%$ of the continuum, but no ^{13}CO or vibrationally excited lines were detected in the spectra of the other H Ae stars.

4. DISCUSSION

The correlation of the CO line/continuum and FWHM with inclination points to an origin in the disks encircling these H Ae

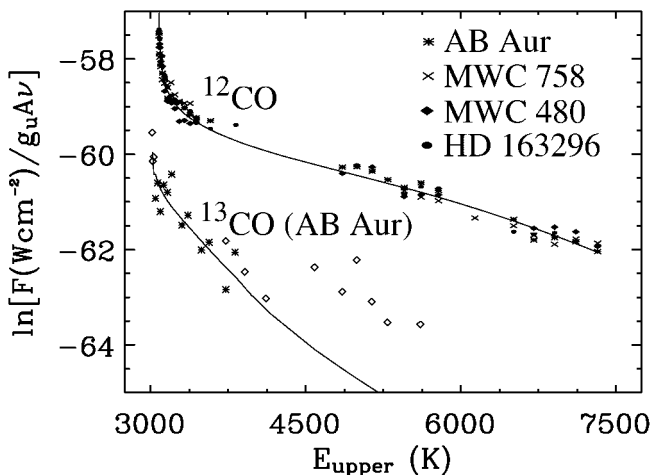


FIG. 3.— ^{12}CO $v = 1 \rightarrow 0$ rotation diagrams, normalized to the inclination angle and distance of AB Aur. ^{13}CO data from AB Aur are also included; upper limits are plotted as open diamonds. The disk model fits, including both thermal emission and resonance fluorescence, are indicated by the solid lines, for $^{12}\text{CO}/^{13}\text{CO} = 80$.

stars. Characteristic radii from the FWHM are 0.5–5 AU, distances at which the disks are optically thick. The CO lines thus arise near the disk surface where both collisional and radiative excitation are possible. Photoexcitation can occur via the $A \leftarrow X$ ($\lambda \sim 145$ – 150 nm) or $v = 1 \leftarrow 0$ ($\lambda \sim 4.7$ μm) bands, but the weakness of any $v = 2-1$, $3-2$ lines suggests that UV pumping is unimportant (Brittain & Rettig 2002). The disk CO emission clearly demands a temperature gradient that increases vertically or $T_{\text{gas}} \neq T_{\text{dust}}$, while the lack of UV excitation is consistent with the “puffed up” inner rim invoked to explain the 2–5 μm emission bump in the SEDs of H Ae star+disk systems (Dullemond 2002 and references therein).

Provided background radiation can be ignored, the line flux F of an optically thin emission line is given by $F = (h\nu_{ul} \times N_u \times A_{ul} \times \Omega)/4\pi$ (W cm^{-2}), where N_u is the upper state column density, ν_{ul} is the line frequency, and Ω is the emitting region solid angle. Plots of $\ln(F/g_u A_{ul} \nu_{ul})$ versus energy (where g_u is the upper state degeneracy) for optically thin, isothermal gas in local thermodynamic equilibrium (LTE) should therefore yield straight lines whose intercept is proportional to $N_{v=1}$ (cm^{-2}) and whose slope is $-1/T_{\text{ex}}$. Disk CO emission, however, produces rotation diagrams that are strongly curved (Fig. 3). Opacity effects can generate such curvature, and while the ^{13}CO detections in AB Aur demonstrate that $\tau(^{12}\text{CO}) > 1$, the substantial temperature gradients known to be present in disks can also produce nonlinear rotation diagrams.

Indeed, two-temperature LTE as well as $\tau \gg 1$ isothermal fits have been used to interpret the CO emission from H Ae (Brittain & Rettig 2002) and TTs (Najita et al. 2003) disks, but more detailed physical models are needed to simultaneously reproduce the rotation diagrams and line profiles and to disentangle opacity from excitation effects. We have therefore generated synthetic spectra using two-dimensional disk temperature/density models (Dullemond 2002, Fig. 1; see also Dominik et al. 2003). Dust and gas emission from 0.6 to 100 AU in regions with $\tau_{\text{dust}} (5 \mu\text{m}) \lesssim 1$ are treated, and to model the spectral lines the CO $v = 0$ rotational levels are assumed to be in LTE with $T_{\text{CO}} = T_{\text{dust}}$. Emission from the $v = 1$ states is driven by collisions and resonance fluorescence. The high critical densities for $v = 1, 2$ and the small $v = 2 \leftarrow 0$ radiative cross sections naturally explain the lack of $v = 2-1$ emission.

The line shapes are examined with a Keplerian disk formalism (Horne & Marsh 1986) assuming $(\text{CO}/\text{H}_2) \sim 10^{-4}$ and the dust opacities in Chiang et al. (2001). The line excess is insensitive to the disk mass since $\tau_{\text{dust}} \gg 1$ and depends primarily on the relative line/continuum optical depths. Any processes that lowers τ_{dust} (grain growth, dust settling) therefore permits smaller CO abundances to be used. With collisions alone, the emission is strongly weighted to the innermost radii since the rates scale steeply with T_{gas} (González-Alfonso et al. 2002). Indeed, to reproduce the ^{12}CO fluxes, the disk must be extended inward to $R < 0.3$ AU, a value inconsistent with the line profiles and K -band interferometry (Eisner et al. 2003). Isothermal fits with $T \sim 800$ K, $N(\text{CO}) = 4 \times 10^{18} \text{ cm}^{-2}$, and an emitting area of 0.5 AU^2 can reproduce the ^{12}CO fluxes but not the line profiles or ^{13}CO relative intensities.

Because hydrostatic disks are flared, resonant scattering of 4.7 μm continuum photons can be important even at large radii, especially from the low-density disk surface where collisional quenching is inefficient (Brittain et al. 2003). To model the observed CO FWHM, we find that 25%–85% of the M -band continuum photons that are resonant with CO must be scattered by a disk with well-mixed gas and dust and that this emission

dominates the CO spectrum at low-to-moderate J . The fluorescent line profiles are strongly J -dependent, and for $J \leq 10$ it is found that the observed line shapes can only be reproduced if scattering to $R \geq 100$ AU is included. Thus, this inner rim must shield moderate disk radii from UV radiation but enable a large fraction of the IR photons from the star and warm dust to bathe the disk surface (Brittain et al. 2003).

Only for the highest excitation lines does the thermal emission dominate, at characteristic radii of 0.65–0.8 AU that are well correlated with but larger than those measured in the 2.2 μm continuum (Monnier & Millan-Gabet 2002; Eisner et al. 2003). While the H I emission profiles demonstrate that gas must be present close to the star (see also Muzerolle et al. 2003), the line shapes and $v = 2 \rightarrow 1/1 \rightarrow 0$ ratios illustrate that CO must be rapidly photodissociated inside the dust sublimation radius.

As Figures 2 and 3 show, the combined collisional excitation and resonance fluorescence yield excellent fits to the CO rotation diagrams and line profiles of HAe disks. In particular, the trend of increasing line width with excitation is well reproduced, as is the much lower apparent excitation temperature for the ^{13}CO emission from AB Aur (Fig. 3). Finally, when corrected for the estimated distances and disk inclination angles, the rotation diagrams of AB Aur, MWC 480/758, and HD 163296 are found to be virtually identical (Fig. 3).

While the dust sublimation radius and hence the line widths of the most highly excited CO transitions are sensitive to the stellar type, since they track the radial position of regions with $T \leq 1400$ –1500 K (Muzerolle et al. 2003), models suggest that the curvature in the CO rotation diagrams primarily reflects the radial temperature *gradients* near the disk photosphere. Beyond 1–2 AU, where the bulk of the moderate- J fluorescent emission arises, these gradients vary only as $L_*^{0.25}$ in simple blackbody models, and so they naturally explain the similar curvatures in Figure 3. In principle, the CO spectra can provide numerical estimates of $T(R)$, but such calculations are beyond the scope of this Letter. Since the disks are highly optically thick at 5 μm , the line/continuum trend with inclination (see Fig. 2) and the similar distance-corrected line intensities further sug-

gest that the disk flaring and CO/dust opacities do not vary strongly among this small sample of HAe stars.

5. FUTURE WORK AND CONCLUSIONS

The spectra presented here demonstrate that CO line emission is a powerful probe of disk surfaces for $R = 0.5$ –50 AU and that detailed fits to the full spectra should be able to constrain the radial temperature and density profiles and provide an independent assessment of disk models based on SEDs. Interestingly, resonant scattering from radii as large as 100 AU is visible in the models of the lowest J lines. The intense M -band continuum is confined to $R < 1$ AU; with coronagraphic spectroscopy of CO, we could thus examine disk morphologies and kinematics with ~ 0.1 resolution on diffraction-limited 8–10 m class telescopes.

Finally, the collisional/IR fluorescence pumping scheme outlined here should excite any molecule with active vibrations. The observations of other species, H_2O and CH_4 for example, with varying excitation properties could therefore be used to provide “local” estimates of the density and temperature near the disk surface through departures from LTE. Thanks to their differing chemical behavior, studies of the orbital phase dependence of the CH_4/CO and $\text{H}_2\text{O}/\text{CO}$ ratios versus velocity might also provide an efficient means of searching for potential planetary embryos, gaps, and/or accretion shocks. As the most abundant molecule after H_2 , the CO lines will clearly be among the strongest emitters. The detection of ^{13}CO in AB Aur indicates that less abundant species can be studied, but only if very high dynamic range, high-resolution spectra are acquired in regions of good atmospheric transparency.

G. A. B. and A. C. A. B. acknowledge support from the NASA *Spitzer Space Telescope* and Origins programs. The data presented herein were obtained at the W. M. Keck Observatory, which is operated as a scientific partnership among the California Institute of Technology, the University of California, and NASA. The Observatory was made possible by the generous financial support of the W. M. Keck Foundation.

REFERENCES

- Beckwith, S., Sargent, A., Chini, R., & Gusten, R. 1990, *AJ*, 99, 924
 Boogert, A. C. A., Blake, G. A., & Tielens, A. G. G. M. 2002a, *ApJ*, 577, 271
 Boogert, A. C. A., Hogerheijde, M. R., & Blake, G. A. 2002b, *ApJ*, 568, 761
 Brittain, S. D., & Rettig, T. W. 2002, *Nature*, 418, 57
 Brittain, S. D., et al. 2003, *ApJ*, 588, 535
 Carr, J. S., Mathieu, R. D., & Najita, J. R. 2001, *ApJ*, 551, 454
 Chavarría, C., et al. 1988, *A&A*, 197, 151
 Chiang, E. I., et al. 2001, *ApJ*, 547, 1077
 Dartois, E., Dutrey, A., & Guilloteau, S. 2003, *A&A*, 399, 773
 Dominik, C., Dullemond, C. P., Waters, L. B. F. M., & Walch, S. 2003, *A&A*, 398, 607
 Dullemond, C. P. 2002, *A&A*, 395, 853
 Eisner, J. A., Lane, B. F., Akeson, R. L., Hillenbrand, L. A., & Sargent, A. I. 2003, *ApJ*, 588, 360
 González-Alfonso, E., et al. 2002, *A&A*, 386, 1074
 Grady, C. A., et al. 2000, *ApJ*, 544, 895
 Hillenbrand, L. A., Strom, S. E., Vrba, F. J., & Keene, J. 1992, *ApJ*, 397, 613
 Horne, K., & Marsh, T. R. 1986, *MNRAS*, 218, 761
 Krist, J. E., Stapelfeldt, K. R., Ménard, F., Padgett, D. L., & Burrows, C. J. 2000, *ApJ*, 538, 793
 Malfait, K., Bogaert, E., & Waelkens, C. 1998, *A&A*, 331, 211
 Mannings, V. G., & Sargent, A. I. 2000, *ApJ*, 529, 391
 Marcy, G. W., Cochran, W. D., & Mayor, M. 2000, in *Protostars and Planets IV*, ed. V. Mannings, A. P. Boss, & S. S. Russell (Tucson: Univ. Arizona Press), 1285
 McLean, I. S., Becklin, E. E., Bendiksen, O., Brims, G., & Canfield, J. 1998, *Proc. SPIE*, 3354, 566
 Monnier, J. D., & Millan-Gabet, R. 2002, *ApJ*, 579, 694
 Muzerolle, J., Calvet, N., Hartmann, L., & D’Alessio, P. 2003, *ApJ*, 597, L149
 Najita, J., Carr, J. S., & Mathieu, R. D. 2003, *ApJ*, 589, 931
 Najita, J., Carr, J. S., & Tokunaga, A. T. 1996, *ApJ*, 456, 292
 Pontoppidan, K. M., et al. 2003, *A&A*, 408, 981
 Rothman, L. S., et al. 1992, *J. Quant. Spectrosc. Radiat. Transfer*, 48, 469
 Shuping, R. Y., Snow, T. P., Chiar, J. E., & Kerr, T. 2000, *ApJ*, 529, 932
 Simon, M., Dutrey, A., & Guilloteau, S. 2000, *ApJ*, 545, 1034
 Skrutskie, M. F., et al. 1990, *AJ*, 99, 1187
 Thi, W. F., et al. 2001, *ApJ*, 561, 1074
 van den Ancker, M. E., de Winter, D., & Tjin A Djie, H. R. E. 1998, *A&A*, 330, 145
 van den Ancker, M. E., et al. 2000, *A&A*, 357, 325